Supplemental Material: Impact of adsorption kinetics on pollutant dispersion in water flowing in nanopores: A Lattice Boltzmann approach to stationary and transient conditions

Zaineb Zaafouri

IFP Energies Nouvelles, 1 & 4 Av. Bois Préau, 92852 Rueil Malmaison, France

Université Grenoble Alpes, CNRS, LIPhy, 38000 Grenoble, France

Guillaume Batôt

IFP Energies Nouvelles, 1 & 4 Av. Bois Préau, 92852 Rueil Malmaison, France

Carlos Nieto-Draghi

IFP Energies Nouvelles, 1 & 4 Av. Bois Préau, 92852 Rueil Malmaison, France

Benoit Coasne

Université Grenoble Alpes, CNRS, LIPhy, 38000 Grenoble, France

Daniela Bauer

IFP Energies Nouvelles, 1 & 4 Av. Bois Préau, 92852 Rueil Malmaison, France

1. Data of the Cooperative Model

Fig. S1 shows the adsorption constant $k'(\Gamma_m)$ of the aggregated monomers m' as a function of the surface concentration Γ'_m, that was used in the simulations. Data was obtained by fitting the experimental data of TX100 adsorption on silica. For more information see (Zaafouri et al. (2020)).

*corresponding authors

Email addresses: benoit.coasne@univ-grenoble-alpes.fr (Benoit Coasne), daniela.bauer@ifpen.fr (Daniela Bauer)

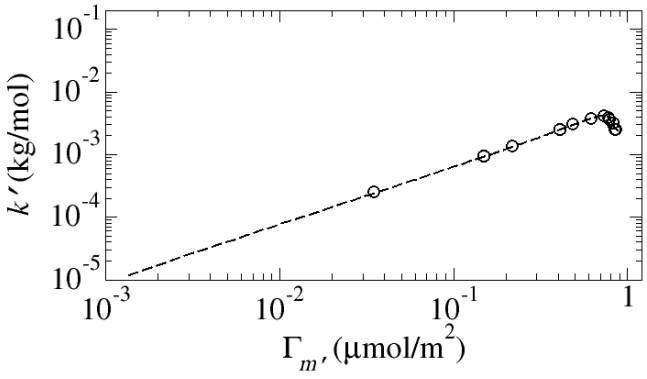

Fig. S1: Adsorption constant $k'(\Gamma_m)$ of the aggregated monomers m' as a function of the surface concentration Γ'_m (dashed line). Data are given for the aggregation coefficient $\beta = 0.5$. Circles correspond to experimental data. color online only

2. Lattice Boltzmann simulation algorithm for the ADE and Stokes

The basis of the Lattice Boltzmann Method (LBM) lies in the specific discretization of the Boltzmann equation. Particle velocities and space are discretized on a regular grid, where nodes are related by the velocity vectors $\mathbf{v}_q$, $q \in [0, q_m]$ and $q_m = 8$ here. Particles are only displaced with velocities $\mathbf{v}_q$. Populations $f_q(\mathbf{r}, t)$ are defined as the density of particles at position $\mathbf{r}$ with velocity $\mathbf{v}_q$. When implementing the Lattice Boltzmann model, the computation of the temporal evolution of the particle density is split in two distinct steps, the propagation and collision step, that are processed individually.

Collision step In this step, distribution functions f_q evolve according to the collision operator Ω, specific for the equation to be solved. Distribution functions f_q are updated as follows:

$$\tilde{f}_q(\mathbf{r}, t) = f_q(\mathbf{r}, t) + \Omega[f(\mathbf{r}, t)]_q \tag{1}$$

where $\tilde{f}_q(\mathbf{r}, t)$ stands for the post-collision distributions.

Propagation step Here, distribution functions f_q are exchanged between neighboring nodes with respect to the velocity set:

$$f_q(\mathbf{r} + \mathbf{v}_q \Delta t, t + \Delta t) = \tilde{f}_q(\mathbf{r}, t) \tag{2}$$

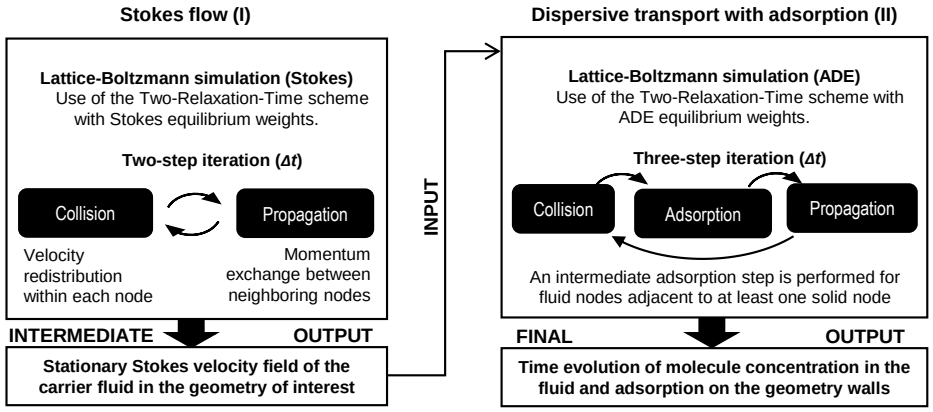

Fig. S2: Description of the different algorithm steps used to study the dispersive transport with adsorption. The first step involves the calculation of the Stokes flow using the LBM-Stokes algorithm. The second step is the Lattice Boltzmann simulation of the advection/diffusion/adsorption processes. The output of the Stokes simulation is the Stokes flow field at equilibrium and it is then used as input for the second step to study the dispersive transport with adsorption.

In the Two Relaxation Time Lattice Boltzmann scheme (TRT) the collision operator contains two different relaxation rates, one for the symmetric and one for the anti-symmetric components. Symmetric components are defined as $f_q^+ = \frac{1}{2}(f_q + f_{\bar{q}})$ while the anti-symmetric components are defined as $f_q^- = \frac{1}{2}(f_q - f_{\bar{q}})$ for $q \in \{1, ..., q_m/2\}$. For $q = 0$, $f_0^+ = f_0$ and $f_0^- = 0$.

The two relaxation parameters are defined as follows: λ^- for all anti-symmetric non-equilibrium components $n_q^- = f_q^- - e_q^-$ and λ^+ for all symmetric non-equilibrium components $n_q^+ = f_q^+ - e_q^+$. Equilibrium components for the zero velocity are given by: $e_0^+ = e_0$ and $e_0^- = 0$.

Eq. 1 is then expressed as (Ginzburg et al. (2010)):

$$\begin{aligned}
\tilde{f}_q(\mathbf{r}, t) &= f_q(\mathbf{r}, t) + \lambda^+ n_q^+ + \lambda^- n_q^- \\
\tilde{f}_{\bar{q}}(\mathbf{r}, t) &= f_{\bar{q}}(\mathbf{r}, t) + \lambda^+ n_q^+ - \lambda^- n_q^- \\
\tilde{f}_0(\mathbf{r}, t) &= f_0(\mathbf{r}, t)(1 + \lambda^+) - \lambda^+ e_0
\end{aligned} \tag{3}$$

with $q \in \{1, .., q_m/2\}$. The LBM-TRT requires the definition of a set of numerical parameters $\Lambda^{\pm}$ and Λ to ensure the stability of the algorithm. These parameters are related to the relaxation parameters $\lambda^{\pm}$ as follows (Ginzburg et al. (2010)):

$$\Lambda = \Lambda^{+}\Lambda^{-} \tag{4}$$

with

$$\Lambda^{\pm} = -(1/2 + 1/\lambda^{\pm}) \tag{5}$$

for $-2 < \lambda^{\pm} < 0$. Values of the latter parameters depend on the equation to be solved. Specificities of the resolution of Stokes equation and the advection-diffusion equation are presented in the following.

2.1. Stokes equation

Stokes equation in the absence of external forces – besides the pressure gradient ∇P inducing the flow – is given by:

$$\begin{aligned} \boldsymbol{\nabla}\mathbf{j} &= 0 \\ \boldsymbol{\nabla}P &= \nu\Delta\mathbf{j} \end{aligned} \tag{6}$$

with $\mathbf{j}$ being the momentum. Equilibrium distributions $e_q^{\pm}$ are defined as (Ginzburg (2007)):

$$\begin{aligned} e_q^{+}(\mathbf{r},t) &= v_s^2\rho(\mathbf{r},t)t_q^* \\ e_q^{-}(\mathbf{r},t) &= t_q^*(\mathbf{j}(\mathbf{r},t).\mathbf{v}_q) \\ e_0^{+}(\mathbf{r},t) &= \rho(\mathbf{r},t) - \sum_{q=1}^{q_m} e_q^{+}(\mathbf{r},t) \\ e_0^{-} &= 0 \end{aligned} \tag{7}$$

where v_s is the sound velocity and t_q^* correspond to isotropic physical weights obeying two constraints:

$$\sum_{q=1}^{q_m} t_q^*\mathbf{v}_{q\alpha}\mathbf{v}_{q\beta} = \delta_{\alpha\beta}\ \forall\alpha,\beta \tag{8}$$

and

$$\sum_{q=1}^{q_m} t_q^*\mathbf{v}_{q\alpha}^2\mathbf{v}_{q\beta}^2 = \frac{1}{3}\ \forall\alpha \neq \beta \tag{9}$$

with $\alpha, \beta \in \{1, 2\}$ and $\delta_{\alpha\beta} = 0$ if $\alpha \neq \beta$ and $\delta_{\alpha\beta} = 1$ if $\alpha = \beta$.

t_q^* take the value $t_q^* = \left\{\frac{1}{3}; \frac{1}{12}\right\}$ for the first (coordinate) and the second (diagonal) neighbor link in the d_2q_9 scheme (Ginzburg (2007)).
The calculation of the equilibrium functions requires to compute the fluid density ρ and the momentum $\mathbf{j}$. They are expressed as (Ginzburg (2007)):

$$\rho(\mathbf{r}, t) = \sum_{q=0}^{q_m} f_q(\mathbf{r}, t) \tag{10}$$

and

$$\mathbf{j}(\mathbf{r}, t) = \sum_{q=1}^{q_m} f_q(\mathbf{r}, t)\mathbf{v}_q \tag{11}$$

Fluid velocity is given by $\boldsymbol{U}(\mathbf{r}, t) = \frac{\mathbf{j}(\mathbf{r},t)}{\rho}$.
In Eq. 6 the pressure is defined as $P = v_s^2\rho$ and the kinematic viscosity as $\nu = \frac{\Lambda^+}{3} = -\frac{1}{3}(\frac{1}{2} + \frac{1}{\lambda^+})$.
v_s is an adjustable positive parameter that must verify the following condition: $v_s^2 < v_s^{max2}$. Based on the stability analysis by Ginzburg (2008), v_s^{max2} must be set to $\frac{1}{3}$. Here, to satisfy this criterion, we choose $v_s^2 = \frac{1}{5}$. In our case, numerical accuracy is obtained by using $\Lambda = 3/16$ (Ginzburg (2008)). We choose $\nu = 1/10$, so $\Lambda^+ = 3/10$ and $\Lambda^- = 10/16$.

At the solid/fluid interface (when $\mathbf{v}_q$ is pointing towards the wall) we applied no-slip boundary conditions via the bounce back rule:

$$f_{\bar{q}}(\mathbf{r}, t + \Delta t) = \tilde{f}_q(\mathbf{r}, t). \tag{12}$$

The inlet/outlet boundary conditions (see Talon et al. (2012)) are given by :

$$f_{\bar{q}}(\mathbf{r}, t+\Delta t) = -\tilde{f}_q(\mathbf{r}, t)+2t_q^*c_s^2\rho_{in}+(2+\lambda^+)n_q^+(\mathbf{r}, t)-6t_q^*v_{qy}j_y(\mathbf{r}, t); \forall \mathbf{r} = (0, y) \tag{13}$$

$$f_{\bar{q}}(\mathbf{r}, t+\Delta t) = -\tilde{f}_q(\mathbf{r}, t)+2t_q^*c_s^2\rho_{out}+(2+\lambda^+)n_q^-(\mathbf{r}, t)-6t_q^*v_{qy}j_y(\mathbf{r}, t); \forall \mathbf{r} = (L_x-1, y) \tag{14}$$

where $c_s^2\rho_{in}$ and $c_s^2\rho_{out}$ correspond to the imposed inlet and outlet pressure. L_x represents the length of the channel. q the link that crosses the boundary, $\tilde{f}_q(\mathbf{r}, t)$ is thus the outgoing distribution after collision.

2.2. Advection-diffusion equation (ADE)

The advection-diffusion equation is given by

$$\frac{\partial c(\mathbf{r},t)}{\partial t} + \boldsymbol{U}.\nabla c(\mathbf{r},t) - D_m \Delta c(\mathbf{r},t) = 0 \tag{15}$$

where c is the solute concentration in the fluid, $\boldsymbol{U}$ the velocity vector and D_m the molecular self-diffusion coefficient. For the sake of clarity, populations used in Eq. 3 are named g_q if the ADE is resolved. Equilibrium components of the d_2q_9 scheme used in Eq. 3 are given by (Ginzburg et al. (2010)):

$$\begin{aligned} e_q^+(\mathbf{r},t) &= c(\mathbf{r},t)E_q^+ \\ e_q^-(\mathbf{r},t) &= c(\mathbf{r},t)E_q^- \\ e_0^+(\mathbf{r},t) &= e_0 = c(\mathbf{r},t)E_0 \\ e_0^-(\mathbf{r},t) &= 0 \end{aligned} \tag{16}$$

with

$$\begin{aligned} E_q^+ &= t_q^* v_e + \frac{t_q^*}{2}(3(\boldsymbol{U}.\mathbf{v}_q)^2 - \boldsymbol{U}^2) \\ E_q^- &= t_q^*(\boldsymbol{U}.\mathbf{v}_q) \\ E_0 &= \left(1 - \sum_{q=1}^{q_m} E_q^+(\mathbf{r},t)\right) \end{aligned} \tag{17}$$

where the diffusion-scale equilibrium parameter v_e is defined as $v_e = D_m/\Lambda^-$. The isotropic weights are set to $t_q^* = \left\{\frac{1}{3}; \frac{1}{12}\right\}$ and $\boldsymbol{U} = \{U_x, U_y\}$ is the advective velocity with $\boldsymbol{U}^2 = U_x^2 + U_y^2$. Ginzburg et al. (2010) stated, that an optimal TRT subclass requires the choice of (Λ^+, Λ^-) such that $\Lambda = \frac{1}{4}$. In the present work, we set $\Lambda^+ = 4$ and $\Lambda^- = 1/16$.

The result of the ADE simulation is the local concentration of the tracer $c(\mathbf{r},t)$ computed at each time step t from:

$$c(\mathbf{r},t) = \sum_{q=0}^{q_m} g_q(\mathbf{r},t). \tag{18}$$

The velocity vector $\boldsymbol{U}$ is computed by means of the resolution of Stokes equation.

No-slip boundary conditions at the solid/fluid interfaces were applied by using the bounce-back condition:

$$g_{\bar{q}}(\mathbf{r}, t + \Delta t) = \tilde{g}_q(\mathbf{r}, t) \tag{19}$$

3. Dispersion coefficient for adsorbing molecules following the Henry isotherm

The analytical resolution of the transport equation including an adsorption term was addressed by Levesque et al. (2012) by means of a statistical physics approach. Based on a stochastic treatment, Levesque et al. (2012) derived an analytic expression of the effective dispersion coefficient. In the long time limit, considering Henry adsorption, the effective dispersion coefficient D_{eff}^{ads}/D_m is given by:

$$\frac{D_{eff}^{ads}}{D_m} = 1 + \frac{Pe^2}{(L_y + 2k_H)^3}\Big[\frac{102L_y{k_H}^2 + 18L_y^2k_H + L_y^3}{210} \quad + \quad \frac{2D_mk_H}{k_D}\Big] \tag{20}$$

where L_y is the pore width, U is the average velocity of the flowing fluid, and D_m is the bulk molecular diffusion coefficient. The adsorption/desorption ratio k_H is related to the adsorption (k_A) and desorption (k_D) rate by $k_H = k_A/k_D$.

4. Comparison of the Henry and the Langmuir adsorption model

The objective of this part is to further investigate the difference between the Henry and the Langmuir adsorption model. In order to separate the effect of the initial concentration c_0 from the influence of k on the time evolution of $D(t)$, $D(t)$ is normalized by its large time limit $D(t \to \infty)$. As can be seen from Fig. S3, the difference between both models becomes more pronounced for larger values of k.

5. Cooperative model for Dirac pulse injection

In this section, we study the impact of cooperative adsorption on the transport induced by Dirac pulse injection. We consider an initial concentration $c_0 = 1000$ and a Peclet number Pe $= 100$. Values of $k'(\Gamma_{m'})$ are

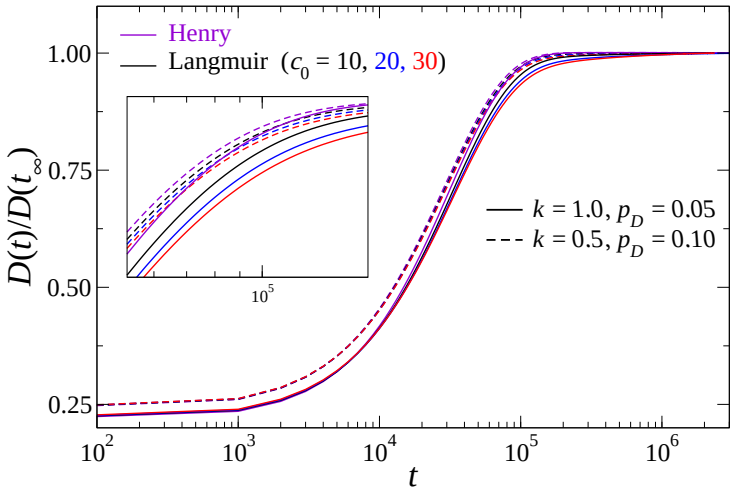

Fig. S3: Temporal evolution of the time derivative of the displacement variance $D(t)$. $D(t)$ is normalized by the effective dispersion coefficient $D(t \to \infty)$. We consider the dispersion of molecules that follow different adsorption models. The solid and dashed lines represent data obtained for adsorption/desorption ratios $k = 1$ and $k = 0.5$. The black, blue and red colors denote Langmuir adsorption configuration for $c_0 = 10$, $c_0 = 20$ and $c_0 = 30$, respectively. The violet curves represent Henry adsorption configuration for $c_0 = 10$. The flowing liquid considered here is characterized by Pe = 25. color online only

given in Fig. S1. Two data sets are considered: $k_H = 2.6 \times 10^{-6}$, k' given in Fig. S1 and $k_{H_1} = 10^3\ k_H$, $k'_1 = 10^3\ k'$. In what follows, we compare the dispersion of adsorbing molecules as obtained for the cooperative model ($c_s = 117\mu$mol/kg and $CMC = 281\mu$mol/kg) and the Henry adsorption model. Fig. S4 shows the time evolution of $D(t)/D_m$ for both models. For the set (k_H, k'), data of the Henry model and the cooperative model perfectly overlap with those obtained for non-adsorbing molecules - i.e. the impact of adsorption on the displacement variance is extremely small. Such a behavior can be explained as follows. After injection, a rapid decrease of the bulk concentration takes place due to dispersion, so that the initially injected concentration ($c_0 = 1000$) reaches a free molecule concentration smaller than c_s. For such very low concentrations, the cooperative model is strictly equivalent to the Henry model and in this case, as the adsorption parameters are extremely low, similar to the passive tracer. For the second parameter set (k_{H_1}, k'_1), D_{ads}^{eff}/D_m increases as predicted by the theoretical model, however, there is also no difference between the two adsorption models. In conclusion, Dirac injection leads to a rapid decrease of the initially injected concentra-

tion below the critical surface concentration c_s. Thus, further investigation of the cooperative model requires the injection of molecules during a longer time period avoiding the dilution of the bulk concentration.

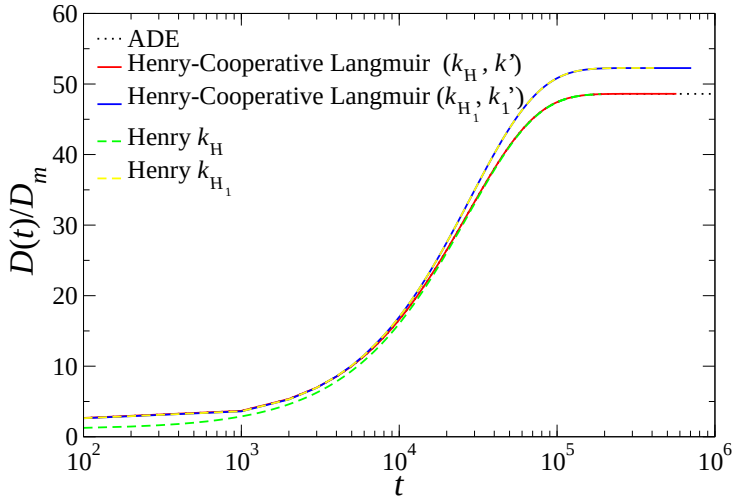

Fig. S4: Time evolution of the time derivative of the displacement variance $D(t)$. $D(t)$ is normalized by the molecular diffusion coefficient D_m of the free tracer molecules. The dotted, solid and dashed lines denote the data for non-adsorbing molecules, molecules obeying the cooperative adsorption model and molecules obeying the Henry adsorption model. The blue and red colors denote the adsorption configuration with the two parameter sets (k_H, k') and ($k_{H_1} = 10^3\ k_H$, $k_1' = 10^3\ k'$), respectively. The green and yellow colors denote systems with k_H and $k_{H_1} = 10^3\ k_H$. The systems considered are characterized by Peclet number Pe = 100, $c_0 = 1000$, $c_s = 117$ and $CMC = 281$. color online only

Ginzburg, I., 2007. Lattice boltzmann modeling with discontinuous collision components: Hydrodynamic and advection-diffusion equations. Journal of Statistical Physics 126 (1), 157–206.

Ginzburg, I., 2008. Consistent lattice boltzmann schemes for the brinkman model of porous flow and infinite chapman-enskog expansion. Physical Review E 77 (6), 066704.

Ginzburg, I., d'Humières, D., Kuzmin, A., 2010. Optimal stability of advection-diffusion lattice boltzmann models with two relaxation times for positive/negative equilibrium. Journal of Statistical Physics 139 (6), 1090–1143.

Levesque, M., Bénichou, O., Voituriez, R., Rotenberg, B., 2012. Taylor dispersion with adsorption and desorption. Physical Review E 86 (3), 036316.

Talon, L., Bauer, D., Gland, N., Youssef, S., Auradou, H., Ginzburg, I., 2012. Assessment of the two relaxation time lattice-boltzmann scheme to simulate stokes flow in porous media. Water Resources Research 48 (4).

Zaafouri, Z., Bauer, D., Batôt, G., Nieto-Draghi, C., Coasne, B., 2020. Cooperative effects dominating the thermodynamics and kinetics of surfactant adsorption in porous media: From lateral interactions to surface aggregation. The Journal of Physical Chemistry B.